1521-0103/348/2/281–292$25.00
THE JOURNAL OF PHARMACOLOGY AND EXPERIMENTAL THERAPEUTICS
Copyright © 2014 by The American Society for Pharmacology and Experimental Therapeutics
http://dx.doi.org/10.1124/jpet.113.210435
J Pharmacol Exp Ther 348:281–292, February 2014

Heat Shock Protein 70 Is Necessary to Improve Mitochondrial Bioenergetics and Reverse Diabetic Sensory Neuropathy following KU-32 Therapy[S]

Jiacheng Ma, Kevin L. Farmer, Pan Pan, Michael J. Urban, Huiping Zhao, Brian S. J. Blagg, and Rick T. Dobrowsky

Department of Pharmacology and Toxicology (J.M., K.L.F., P.P. M.J.U., R.T.D.) and Department of Medicinal Chemistry (H.Z., B.S.J.B.), The University of Kansas, Lawrence, Kansas

Received October 13, 2013; accepted November 20, 2013

ABSTRACT

Impaired neuronal mitochondrial bioenergetics contributes to the pathophysiologic progression of diabetic peripheral neuropathy (DPN) and may be a focal point for disease management. We have demonstrated that modulating heat shock protein (Hsp) 90 and Hsp70 with the small-molecule drug KU-32 ameliorates psychosensory, electrophysiologic, morphologic, and bioenergetic deficits of DPN in animal models of type 1 diabetes. The current study used mouse models of type 1 and type 2 diabetes to determine the relationship of changes in sensory neuron mitochondrial bioenergetics to the onset of and recovery from DPN. The onset of DPN showed a tight temporal correlation with a decrease in mitochondrial bioenergetics in a genetic model of type 2 diabetes. In contrast, sensory hypoalgesia developed 10 weeks before the occurrence of significant declines in sensory neuron mitochondrial bioenergetics in the type 1 model. KU-32 therapy improved mitochondrial bioenergetics in both the type 1 and type 2 models, and this tightly correlated with a decrease in DPN. Mechanistically, improved mitochondrial function following KU-32 therapy required Hsp70, since the drug was ineffective in diabetic Hsp70 knockout mice. Our data indicate that changes in mitochondrial bioenergetics may rapidly contribute to nerve dysfunction in type 2 diabetes, but not type 1 diabetes, and that modulating Hsp70 offers an effective approach toward correcting sensory neuron bioenergetic deficits and DPN in both type 1 and type 2 diabetes.

Introduction

Diabetic peripheral neuropathy (DPN) is experienced by a majority of patients with type 1 or type 2 diabetes (Callaghan et al., 2012). The development of DPN is associated with a small-fiber neuropathy resulting from dysfunction of unmyelinated or thinly myelinated sensory fibers and the gradual degeneration of larger myelinated fibers. Although numerous pathologic mechanisms contribute to DPN (Farmer et al., 2012), altered mitochondrial bioenergetics (mtBE) may be a central facilitator in its development (Fernyhough et al., 2010). For example, mitochondrial function is impaired in adult sensory neurons or dorsal root ganglia isolated from diabetic rats (Huang et al., 2003, 2005; Chowdhury et al., 2010; Akude et al., 2011). Additionally, in-depth bioenergetic analysis of adult sensory neurons isolated from models of type 1 diabetic mice (Urban et al., 2012) or rats (Chowdhury et al., 2012) found substantive decreases in mtBE. However, since the etiologic development of DPN in type 1 and type 2 diabetes does not necessarily share identical mechanisms, it is unclear whether deficits in mtBE may have a kinetically similar relationship to the onset of sensory hypoalgesia that is symptomatic of DPN. Moreover, the efficacy of interventional therapies is also not identical in patients with type 1 versus type 2 diabetes. For example, tight control of blood glucose more effectively ameliorates DPN in patients with type 1 diabetes (Callaghan et al., 2012). Similarly, enalapril improved nerve blood flow and electrophysiology in a type 1 diabetic rat model (Coppey et al., 2006), but had modest effects in diabetic Zucker fatty rats, a type 2 model (Oltman et al., 2008). These results underscore that an effective therapy for DPN should be equally efficacious regardless of the underlying diabetic phenotype. To this end, we have been exploring the potential of pharmacologically manipulating molecular chaperones for treating DPN.

Heat shock protein (Hsp) 90 and Hsp70 are molecular chaperones that are critical for folding nascent proteins into their biologically active conformations (Evans et al., 2010). Hsp90 contains N- and C-terminal ATP-binding domains and

This work was supported by grants from the Juvenile Diabetes Research Foundation (to R.T.D.); the National Institutes of Health National Institute of Neurological Disorders and Stroke [Grant NS054847] (to R.T.D.); National Institutes of Health National Institute of Diabetes and Digestive and Kidney Diseases [Grant DK095911] (to R.T.D.); National Institutes of Health National Cancer Institute [Grants CA120458 and CA109265] (to B.S.J.B.); and the National Institute of Neurological Disorders and Stroke [Grant NS075311] (to B.S.J.B. and R.T.D.).
dx.doi.org/10.1124/jpet.113.210435.
[S] This article has supplemental material available at jpet.aspetjournals.org.

ABBREVIATIONS: DPN, diabetic peripheral neuropathy; DRG, dorsal root ganglia; FBG, fasting blood glucose; FCCP, carbonylcyanide-4-(trifluoromethoxy)-phenylhydrazone; HbA_{1c}, glycated hemoglobin; Hsp, heat shock protein; KO, knockout; MRC, maximum respiratory capacity; mtBE, mitochondrial bioenergetics; MNCV, motor nerve conduction velocity; OCR, oxygen consumption rate; PCR, polymerase chain reaction; RCR, respiratory control ratio; SNCV, sensory nerve conduction velocity; SRC, spare respiratory capacity; STZ, streptozotocin; WT, wild-type.

has intrinsic ATPase activity. Because pharmacologic agents that inhibit the N- or C-terminal ATPase activity can prevent protein folding, inhibiting Hsp90 is an attractive target for treating malignancies, as many oncoproteins require Hsp90 for proper folding (Peterson and Blagg, 2009). However, Hsp90 also binds the transcription factor, heat shock factor 1. Upon exposure to Hsp90 inhibitors, heat shock factor 1 dissociates from Hsp90, translocates to the nucleus, and upregulates a heat shock response that promotes synthesis of cytoprotective antioxidant genes and chaperones, such as Hsp70. This response can antagonize the desired goal of cytotoxicity in treating cancers. On the other hand, inducing the heat shock response can increase molecular chaperones and decrease misfolded protein aggregates. Thus, stimulating this aspect of Hsp90 biology may have utility for treating neurodegenerative diseases (Morimoto, 2011; Zhao et al., 2012). However, developing an effective Hsp90 inhibitor for treating neurodegeneration requires establishing a therapeutic window that leads to upregulation of cytoprotective chaperones, such as Hsp70, in the absence of client protein degradation that can antagonize the protective heat shock response.

Novobiocin is the prototypic ligand that binds to the C-terminal site of Hsp90, and systematic modification of novobiocin identified KU-32 (Fig. 1A) as a neuroprotective lead compound that exhibits a 500-fold divergence of Hsp70 induction from client protein degradation (Urban et al., 2010). This divergence provides an excellent therapeutic window to promote neuroprotection in the absence of toxicity; weekly administration of KU-32 reversed psychosensory, electrophysiologic, bioenergetic, and morphologic indices of DPN in diabetic mice (Urban et al., 2010, 2012). Mechanistically, KU-32 binds Hsp90 directly (Matts et al., 2011), but the drug's neuroprotective efficacy

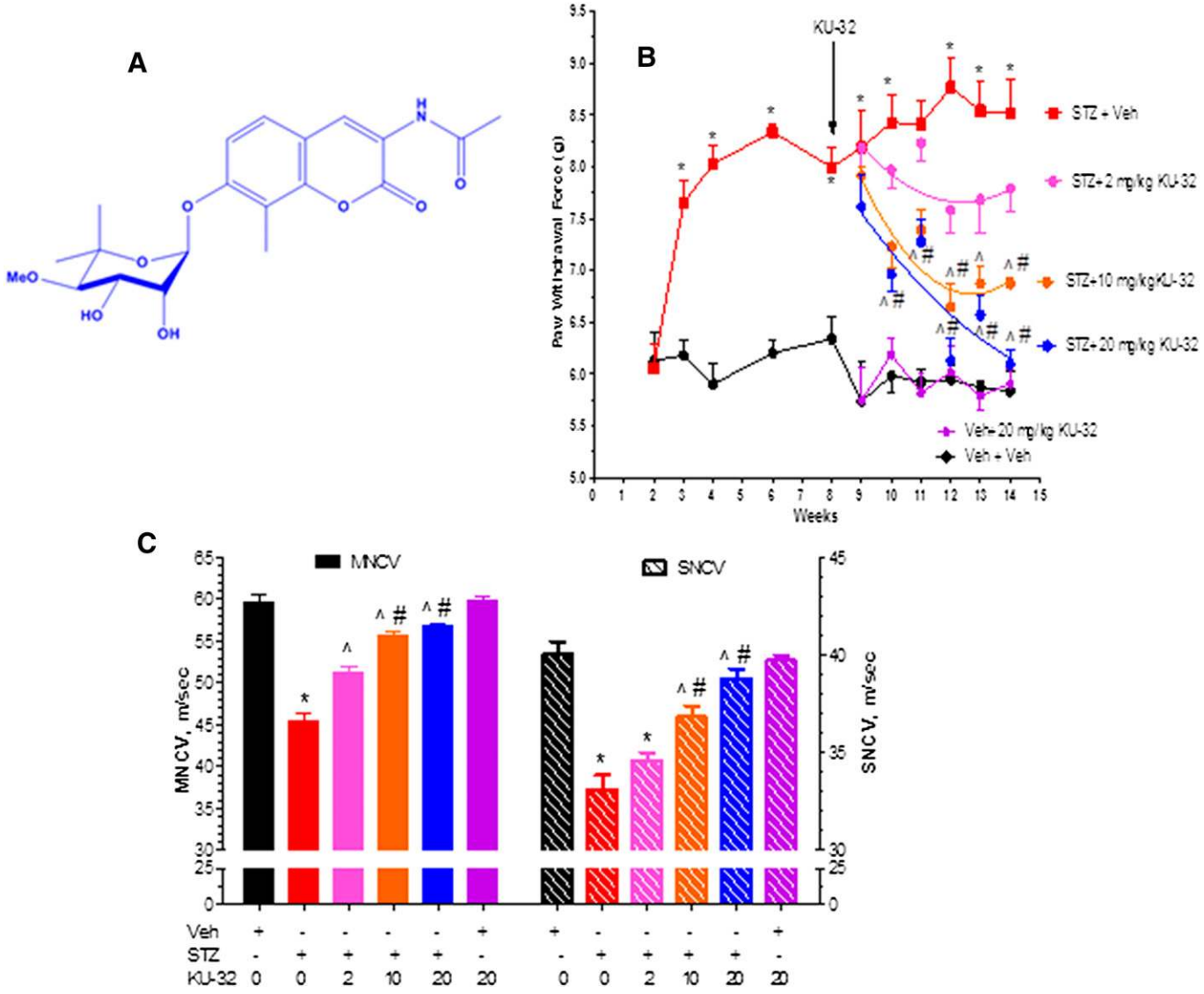

Fig. 1. Dose response of KU-32 in improving mechanical hypoalgesia and NCV deficits in diabetic Swiss Webster mice. (A) Structure of KU-32. (B) Swiss Webster mice were rendered diabetic with STZ and mechanical sensitivity was assessed at the indicated weeks. After 8 weeks of diabetes, mice were treated once per week with 2, 10, or 20 mg/kg KU-32 for 6 weeks and mechanical sensitivity measured weekly. One group of nondiabetic mice was treated with only 20 mg/kg KU-32 as a control. *$P < 0.05$ versus time-matched vehicle (Veh) + Veh; ^$P < 0.05$ versus time-matched STZ + Veh; #$P < 0.05$ versus time-matched STZ+ 2 mg/kg KU-32. (C) Effect of 6 weeks of KU-32 therapy on MNCV and SNCV. *$P < 0.05$ versus Veh + Veh; ^$P < 0.05$ versus STZ + Veh; #$P < 0.05$ versus STZ + 2 mg/kg KU-32.

depends upon the downstream action of Hsp70 (Urban et al., 2010; Li et al., 2012).

The current study sought to determine whether deficits in mtBE in models of type 1 and type 2 diabetes show a similar relationship to the temporal onset of sensory hypoalgesia and ascertain if KU-32 improves mtBE and reverses DPN in an Hsp70-dependent manner. Our results indicate that the development of a sensory hypoalgesia preceded substantial changes in mtBE in type 1 diabetic mice. In contrast, the onset of mitochondrial dysfunction and sensory hypoalgesia were tightly correlated in type 2 diabetic mice. KU-32 improved the bioenergetic profile of sensory neurons in an Hsp70-dependent manner and effectively reversed insensate DPN in both diabetic models. These data provide novel insight into the role of mitochondrial dysfunction in the onset of insensate DPN and indicate that Hsp70 can have beneficial effects on mtBE.

Materials and Methods

Streptozotocin (STZ), carbonylcyanide-4-(trifluoromethoxy)-phenylhydrazone (FCCP), oligomycin, rotenone, antimycin A, Percoll, and poly(DL)ornithine were obtained from Sigma-Aldrich (St. Louis, MO). KU-32, [*N*-(7-((2*R*,3*R*,4*S*,5*R*)-3,4-dihydroxy-5-methoxy-6,6-dimethyl-tetrahydro-2*H*-pyran-2-yloxy)-8-methyl-2-oxo-2*H*-chromen-3-yl)acetamide] and trideutero KU-32 were synthesized and structural purity (>95%) verified as described previously (Huang and Blagg, 2007). Collagenase and laminin were purchased from Gibco/Invitrogen (Carlsbad, CA).

Animals. Male and female wild-type (WT) C57Bl/6 and Hsp70.1/70.3 double knockout (KO) mice on a C57Bl/6 background (Hsp70 KO) were used in the study and obtained from in-house breeding colonies (Urban et al., 2010). Male Swiss Webster mice were purchased from Harlan Laboratories (Indianapolis, IN). As a model of type 1 diabetes, 8-week-old male and female mice were fasted for 6 hours and rendered diabetic with an intraperitoneal injection of STZ (100 mg/kg) given on two consecutive days. One week after the second injection, mice were fasted as above, blood was obtained from the tail vein, and animals with fasting blood glucose (FBG) ≥ 290 mg/dl (16 mM) were deemed diabetic.

To model type 2 diabetes, heterozygous BKS.Cg-Dock7m$^{+/+}$ Lepr^{db}/J mice were acquired from The Jackson Laboratory (Bar Harbor, ME) to generate animals homozygous (Lepr$^{db/db}$) for the *lepr* mutation. Heterozygous (Lepr$^{db/+}$) mice served as controls. At ~4–6 weeks of age, the Lepr$^{db/db}$ mice became identifiably obese and exhibited elevated FBG compared with their heterozygous littermates. Similar numbers of male and female animals between the genotypes were enrolled in the study when they were 8 weeks old.

All animals were maintained on a 12-hour light/dark cycle with ad libitum access to water and Purina 5001 rodent chow. Preliminary dose-response studies indicated that after 8 weeks of diabetes, once a week dosing of 20 mg/kg KU-32 administered intraperitoneally in 0.2 ml of 0.1 M Captisol (β-cyclodextrin sulfobutylethers; CyDex Pharmaceuticals, Lenexa, KS) gave maximal recovery of mechanical hypoalgesia (Fig. 1B) and nerve conduction velocity deficits (Fig. 1C). All subsequent studies were performed using a once per week 20 mg/kg dosing of the drug. At the termination of each study and prior to sacrifice of the animals, FBG and hemoglobin A_{1c} levels (A1c Now^{+}) were determined. All animal procedures were performed in accordance with protocols approved by the Institutional Animal Care and Use Committee and in compliance with standards and regulations for the care and use of laboratory rodents set by the National Institutes of Health.

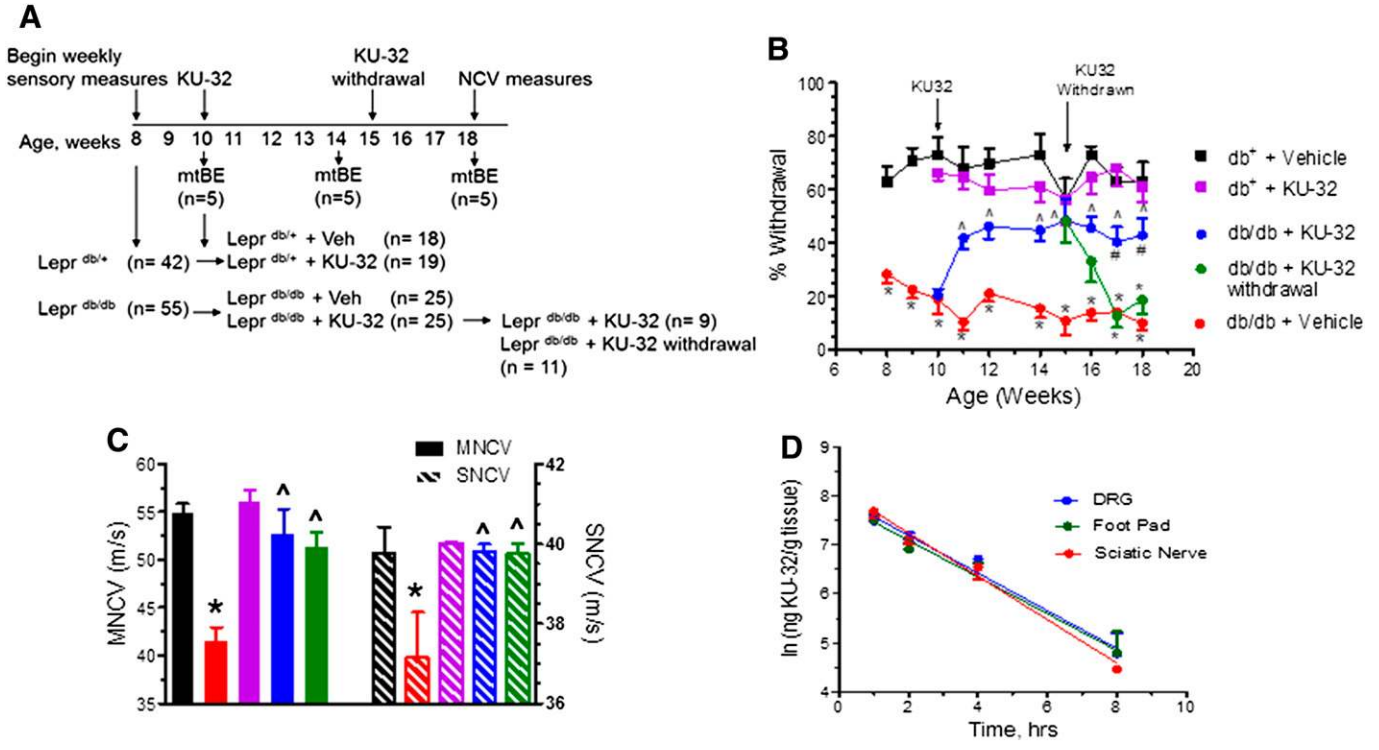

Fig. 2. KU-32 improves mechanical hypoalgesia and NCV deficits in Lepr$^{db/db}$ mice. (A) Scheme of the study design using the Lepr$^{db/db}$ and Lepr$^{db/+}$ mice. (B) Mechanical hypoalgesia was assessed in the Lepr$^{db/db}$ and Lepr$^{db/+}$ mice at the indicated age and weekly KU-32 therapy initiated at 10 weeks of age. KU-32 was then withdrawn in a subgroup of these mice after 4 weeks of treatment. *$P < 0.05$ versus time-matched Lepr$^{db/+}$ + vehicle (Veh); ^$P < 0.05$ versus Lepr$^{db/db}$ + Veh; # =$P < 0.05$ versus Lepr$^{db/db}$ + KU-32 withdrawal. (C) The effect of genotype and treatments on MNCV (solid bars) and SNCV (striped bars) at 18 weeks. Group colors are the same as indicated in (B). *$P < 0.05$ versus time-matched Lepr$^{db/+}$; ^$P < 0.05$ versus Lepr$^{db/db}$ + Veh. (D) Pharmacokinetic analysis of KU-32 uptake in DRG, sciatic nerve, and foot pad.

Psychosensory and Electrophysiologic Analyses. Mechanical sensitivity was assessed in Lepr$^{db/db}$ mice using a nylon Semmes-Weinstein von Frey monofilament (Stoelting, Wood Dale, IL). The filament that possesses a buckling force of 1.4*g* was applied to the plantar surface of the right and left hind paw. A positive response was recorded after lifting or flinching of the animal's paw. This procedure consisted of six trials, which alternated between right and left hind paws. The percent response was obtained by determining the number of withdrawals in response to 12 separate monofilament applications (Jack et al., 2011). Alternatively, mechanical sensitivity was assessed in the type 1 animal models using a Dynamic Plantar Aesthesiometer (Stoelting Inc.) fitted with a stiff monofilament that was applied to the plantar surface at an upward force of 10*g* in the Swiss Webster mice or 8*g* for the C57Bl/6 and Hsp70 KO mice. Thermal sensitivity was assessed by paw withdrawal latency to a ramping, focal heat using a Hargreaves Analgesiometer (Stoelting Inc.) (Urban et al., 2010). Responses from each animal were measured four times on alternate feet and averaged. Sensory assessments were performed once a week at approximately the same time of day. In animals treated with KU-32, sensory measures were taken 1 week after drug administration. At select time points, animals were anesthetized prior to measuring motor and sensory nerve conduction velocities (MNCV and SNCV, respectively) as previously described (McGuire et al., 2009). Animals were then euthanized prior to tissue collection.

Isolation of Adult Sensory Neurons. Adult sensory neurons were isolated from L_4–L_6 dorsal root ganglia (DRG) of three to five mice per treatment with minor modifications (Delree et al., 1989; Urban et al., 2012). After removing connective tissue and trimming, the cleaned ganglia were maintained in 1 ml of serum-free Ham's F10 medium at 37°C and dissociated with 1 ml of 1.25% collagenase for 45 minutes, followed by a secondary digestion with 1 ml of 2% trypsin for 30 minutes. Cells were isolated by centrifugation at 1000 × *g* for 5 minutes, and the pellet was further dissociated by triturating in F10 medium with a fire-polished glass pipette. The cell suspension was layered on a 10-ml gradient of sterile iso-osmotic Percoll and centrifuged at 800*g* for 20 minutes. The cell pellet was resuspended in fresh F10 medium, passed through a 40-μm nylon mesh (Mt. Baker Bio, Everett, WA), and the filter washed with 5 ml of serum-free medium. The cells in the filtrate were recovered by centrifugation and resuspended in maintenance medium: Ham's F10 medium (6.1 mM glucose) containing 50 ng/ml nerve growth factor and 1 ng/ml neurotrophin 3 and N2 supplement without insulin (Invitrogen, Carlsbad, CA). Neurons were plated onto poly(DL)ornithine (0.5 mg/ml overnight)/laminin (2 mg/ml for 3 hours)–coated 96-well plates at 5000–8000 cells per well. Neurons from control and diabetic animals were incubated in maintenance medium for 1 day prior to use in the bioenergetic analysis on day 2 in vitro.

Mitochondrial Bioenergetic Assessment. Oxygen consumption rate (OCR) was assessed in intact lumbar DRG sensory neurons using an XF96 Extracellular Flux Analyzer (Seahorse Biosciences, North Billerica, MA). The maintenance medium was changed 1 hour before starting the assay to unbuffered Dulbecco's modified Eagle's medium supplemented with 1 mM pyruvate and 5.5 mM D-glucose and the cells incubated at 37°C. The plate was introduced into the XF96 analyzer, a 3-minute mix cycle used to oxygenate the medium, and respiration was assessed in a 4-minute measurement cycle. As a general description of a mitochondrial stress assay, the initial rates provide a measure of the basal OCR prior to assessing mitochondrial dysfunction using respiratory chain poisons (Brand and Nicholls, 2011). The portion of basal OCR that is coupled to ATP synthesis was estimated by the decrease in OCR following addition of the ATP synthase inhibitor, oligomycin (1 μg/ml). The residual OCR that persists after oligomycin treatment is from uncoupled respiration (proton leak). Next, maximal respiratory capacity (MRC) was assessed following dissipation of the proton gradient across the inner mitochondrial membrane with the protonophore FCCP (1 μM). Nonmitochondrial respiration was then assessed by coinjection of 1 μM rotenone or rotenone + 1 μM antimycin A.

After the respiratory measures, the cells were harvested and OCR values were normalized to the total protein content of each well. ATP-linked respiration, proton leak, maximal respiratory capacity, spare respiratory capacity, and respiratory control ratio were determined as described previously (Brand and Nicholls, 2011; Chowdhury et al., 2012).

In Vivo Pharmacokinetics. Mice were fasted for 4 hours and Captisol or 20 mg/kg KU-32 given via oral gavage. After 1 hour, food was given ad libitum, the animals sacrificed at the indicated time, and

TABLE 1
Weight, FBG, glycated hemoglobin, and thermal latencies of Lepr$^{db/+}$ and Lepr$^{db/db}$ mice

Week	Group	Weight	*n*	FBG	*n*	HbA_{1c}	Latency[b]	*n*
		g		*mg/dl*		*% (mmol/mol)*[a]	*sec*	
10	*db*$^+$ + Veh	24.8 ± 1.2	5	135 ± 45	5	—	3.5 ± 0.8	5
	db$^+$ + KU-32	24.0 ± 2.1	5	144 ± 14	5	—	4.9 ± 1.4	5
	db/db + Veh	46.6 ± 2.7*	5	317 ± 108*	12	—	4.3 ± 0.3	7
	db/db + KU-32	42.1 ± 4.0*	10	357 ± 111*	23	—	4.3 ± 0.6	15
12	*db*$^+$ + Veh	25.0 ± 3.6	20	124 ± 17	5	—	4.5 ± 1.3	5
	db$^+$ + KU-32	26.1 ± 3.4	22	129 ± 20	5	—	4.4 ± 0.8	5
	db/db + Veh	46.5 ± 5.3*	18	478 ± 98*	18	—	4.9 ± 0.7	7
	db/db + KU-32	45.7 ± 4.0*	37	475 ± 102*	37	—	4.2 ± 0.7	15
14	*db*$^+$ + Veh	25.8 ± 3.6	20	130 ± 21	10	—	4.5 ± 0.9	5
	db$^+$ + KU-32	26.8 ± 3.4	22	118 ± 36	9	—	4.8 ± 0.9	5
	db/db + Veh	48.7 ± 5.6*	18	496 ± 70*	18	—	5.2 ± 0.9	7
	db/db + KU-32	48.4 ± 4.8*	37	518 ± 89*	37	—	4.4 ± 0.9	15
16	*db*$^+$ + Veh	27.8 ± 4.7	10	139 ± 26	5	—	5 ± 0.7	5
	db$^+$ + KU-32	26.8 ± 3.0	8	144 ± 29	5	—	5.2 ± 1.4	5
	db/db + Veh	49.1 ± 5.0*	10	533 ± 61*	13	—	4.9 ± 0.9	7
	db/db + KU-32	49.4 ± 6.5*	12	506 ± 103*	13	—	4.9 ± 0.9	8
	db/db + KU-32 withdrawal	50.6 ± 7.0*	11	501 ± 73*	16	—	5.5 ± 1.0	7
18	*db*$^+$ + Veh	28.0 ± 5.0	10	122 ± 17	5	4.3 ± 0.1 (23 ± 1.1)	5.2 ± 0.6	5
	db$^+$ + KU-32	26.9 ± 3.6	8	137 ± 33	5	4.4 ± 0.1 (24 ± 1.1)	4.8 ± 0.2	5
	db/db + Veh	48.8 ± 5.8*	10	499 ± 78*	10	10.8 ± 0.5* (95 ± 5.6)	4.9 ± 0.7	6
	db/db + KU-32	50.1 ± 8.2*	12	504 ± 90*	12	10.3 ± 0.4* (89 ± 4.6)	5.5 ± 1.3	8
	db/db + KU-32 withdrawal	51.4 ± 8.4*	11	495 ± 54*	11	10.5 ± 0.4* (91 ± 4.2)	5.4 ± 0.6	7

Veh, vehicle.
[a]mmol of HbA_{1c}/mol of hemoglobin.
[b]Paw withdrawal latency to thermal stimuli.
*$P < 0.05$ versus *db*$^+$ + Veh.

lumbar dorsal root ganglia, sciatic nerve, and plantar foot pads harvested and rapidly frozen on dry ice. Tissues were minced, homogenized in water by sonication (25 mg/g water), and spiked with 50 ng/ml trideutero KU-32 as the internal standard. The homogenate was extracted with 1 ml of *t*-butyl methyl ether and centrifuged. An aliquot (0.95 ml) of the supernatant was recovered and evaporated to dryness, and the resulting residue was resuspended in 0.05 ml of 20% CH_3CN. After a second centrifugation, 0.045 ml was transferred to autosampler vials. Chromatographic separation was performed using a 5-micron Agilent Zorbax SB C18 column (2.1 × 50 mm; Santa Clara, CA) and a linear gradient of CH_3CN:H_2O:formic acid (5:95:0.1) to CH_3CN:H_2O:formic acid (95:5.0:0.1) at a flow rate of 0.30 ml/min. The effluent was introduced to a Sciex API3200 Linear Ion Trap detector (Framingham, MA) using turbo ion spray in the positive ion mode. Linear calibration curves were constructed in each tissue matrix over a range of 0–1000 ng/ml, and analyte recoveries ranged from 65% to 75%.

Mitochondrial Copy Number. Real-time polymerase chain reaction (PCR) was used to measure mitochondrial copy number using primers for murine cytochrome *b*, cytochrome *c* oxidase subunit II (COII, mitochondrial genes), and β-actin (nuclear gene) (Santos et al., 2011). Forward and reverse primer sequences for mouse cytochrome *b* were 5'-GCAACCTTGACCCGATTCTTCGC-3' and 5'-TGAACGATTGCTAGGGCCGCG-3'. Forward and reverse primer sequences for mouse COII were 5'-ATTGCCCTCCCCT-CTCTACGCA-3' and 5'-CGTAGCTTCAG-TATCATTGGTGCCC-3'. PCR was performed using 25–50 ng of genomic DNA, 200 nM concentration of each primer, and the SYBR Green PCR master mix from Applied Biosystems (Grand Island, NY). Products were amplified following DNA denaturation at 95°C for 5 minutes followed by 35 cycles at 95°C for 15s, 62°C for 30s, 72°C for 30s, and a final extension at 72°C for 5 minutes. Melting curve analysis and gel electrophoresis verified the specific amplification of the expected product. Differences in gene expression were determined after normalization to β-actin using the ΔΔC(T) method.

Statistical Analysis. Student's *t* tests, one-way analysis of variance (ANOVA), and repeated measures one-way ANOVA were applied for between-group comparisons. Post hoc analyses were conducted using Tukey's test, and nonparametric data were analyzed with a Kruskal-Wallis and Dunn's test. All data are presented as mean ± S.E.M.

Results

KU-32 Reverses DPN in Lepr$^{db/db}$ Mice

Beginning at 8 weeks of age, FBG, body weight, and psychosensory measures were assessed weekly in the Lepr$^{db/db}$ and Lepr^{db+} mice. Each genotype was subdivided into two groups at 10 weeks of age and given a weekly injection of KU-32 or Captisol for up to 8 weeks (Fig. 2A). After 4 weeks of drug therapy, a subgroup of the KU-32-treated Lepr$^{db/db}$ mice was administered Captisol for the final 4 weeks to investigate the effects of drug withdrawal. To examine the effect of diabetes and drug treatment on mitochondrial bioenergetic (mtBE), sensory neurons were isolated from five mice prior to drug treatment and at 4 and 8 weeks after administering KU-32.

Consistent with the onset of type 2 diabetes, the Lepr$^{db/db}$ mice showed significant increases in total body weight and FBG and at 18 weeks of age had elevated glycated hemoglobin levels compared with aged-matched Lepr$^{db/+}$ mice (Table 1). However, treatment with KU-32 did not affect any of these parameters in either genotype, nor did it improve glucose disposal following a 3-hour glucose tolerance test (6-hour fast and 0.5-g glucose given intraperitoneally; data not shown).

By 8 weeks of age, the Lepr$^{db/db}$ mice showed a significantly lower percent withdrawal response to a von Frey hair indicative of a mechanical hypoalgesia (Fig. 2B). In agreement with a prior study (Wright et al., 2007), the Lepr$^{db/db}$ mice did not develop a thermal hypoalgesia (Table 1) and did not show a significant decrease in intra-epidermal nerve fiber density in the foot pad at 18 weeks of age (data not shown). Weekly administration of KU-32 significantly improved mechanical sensitivity in the Lepr$^{db/db}$ mice, but had no effect on the Lepr$^{db/+}$ mice. MNCV and SNCV decreased significantly in the untreated 18-week-old Lepr$^{db/db}$ mice, and KU-32 therapy improved these electrophysiologic deficits (Fig. 2C).

After 4 weeks of KU-32 therapy, drug withdrawal led to a gradual redevelopment of the mechanical hypoalgesia. In contrast, MNCV and SNCV rates remained similar to those observed in the Lepr$^{db/db}$ mice that received the drug continuously. Although the reason for this distinction is unclear, it is not related to differences in the rate of drug clearance since pharmacokinetic analysis showed that KU-32 is rapidly distributed to and quickly cleared from dorsal root

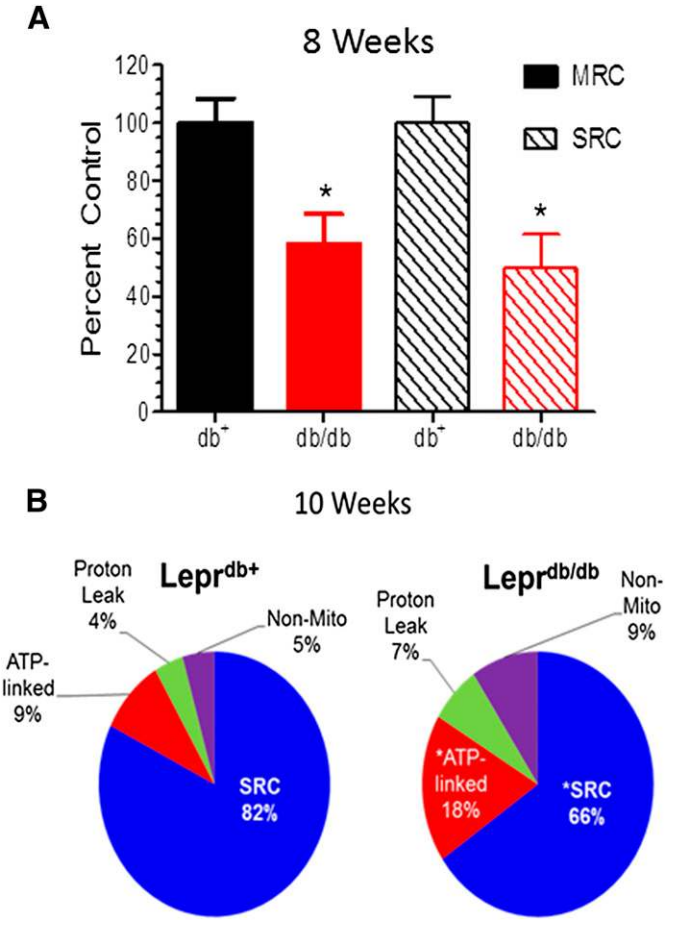

Fig. 3. Deficits in mitochondrial bioenergetics in Lepr$^{db/db}$ mice correlate with the development of mechanical hypoalgesia. Sensory neurons were obtained from 8–10-week-old Lepr$^{db/db}$ and Lepr$^{db/+}$ mice, cultured for 2 days, and mtBE assessed using an XF96 Extracellular Flux Analyzer. (A) MRC and SRC are significantly decreased in 8-week-old Lepr$^{db/db}$ mice compared with age-matched Lepr$^{db/+}$ mice. Respiratory parameters are expressed as the percent of control using values from the Lepr$^{db/+}$ mice. (B) Ten-week-old Lepr$^{db/db}$ mice have a significant decrease in SRC and an increase in ATP-linked and nonmitochondrial respiration compared with age-matched Lepr$^{db/+}$ mice. *$P < 0.05$ versus Lepr$^{db/+}$ + vehicle (Veh). Respiratory parameters are expressed as the percent of the MRC in each genotype.

ganglia, sciatic nerve, and plantar foot pads, with a half-life of 1.5–2 hours (Fig. 2D).

Diabetes-Induced Hypoalgesia Coincides with Decreased Mitochondrial Function in Lepr$^{db/db}$ Mice

The L_4–L_6 lumbar ganglia provide the cell bodies for the motor and sensory fibers that are affected in DPN and whose physiology was improved by KU-32. To determine whether the improvement in psychosensory function and NCV was associated with a change in mtBE, sensory neurons were isolated from these ganglia at 6, 8, 10, 14, and 18 weeks of age. The neurons were cultured in vitro for 2 days and the OCR was determined for 2 hours in the intact cells (Zhang et al., 2012).

At 6 weeks of age, Lepr$^{db/db}$ mice showed a modest decline in maximal respiratory capacity and spare respiratory capacity (SRC), but these parameters were significantly decreased by 8 weeks (Fig. 3A) and 10 weeks (Fig. 3B) of age. To gain broader insight into the effect of diabetes on cellular respiration, the ATP-linked OCR, proton leak, SRC, and nonmitochondrial OCR were expressed as a percent of the MRC (Fig. 3B). At 10 weeks of age, Lepr$^{db/db}$ showed a significant decrease in SRC and an increase in proton leak, ATP-linked OCR, and nonmitochondrial respiration, consistent with an overall alteration in mtBE.

KU-32 Therapy Improves mtBE and Sensory Hypoalgesia in Lepr$^{db/db}$ Mice. Deficits in mtBE worsened by 14 weeks of age (Fig. 4, A and B) and while the extent of ATP-linked and nonmitochondrial respiration increased, SRC declined between 10 and 14 weeks of age (compare Figs. 3B

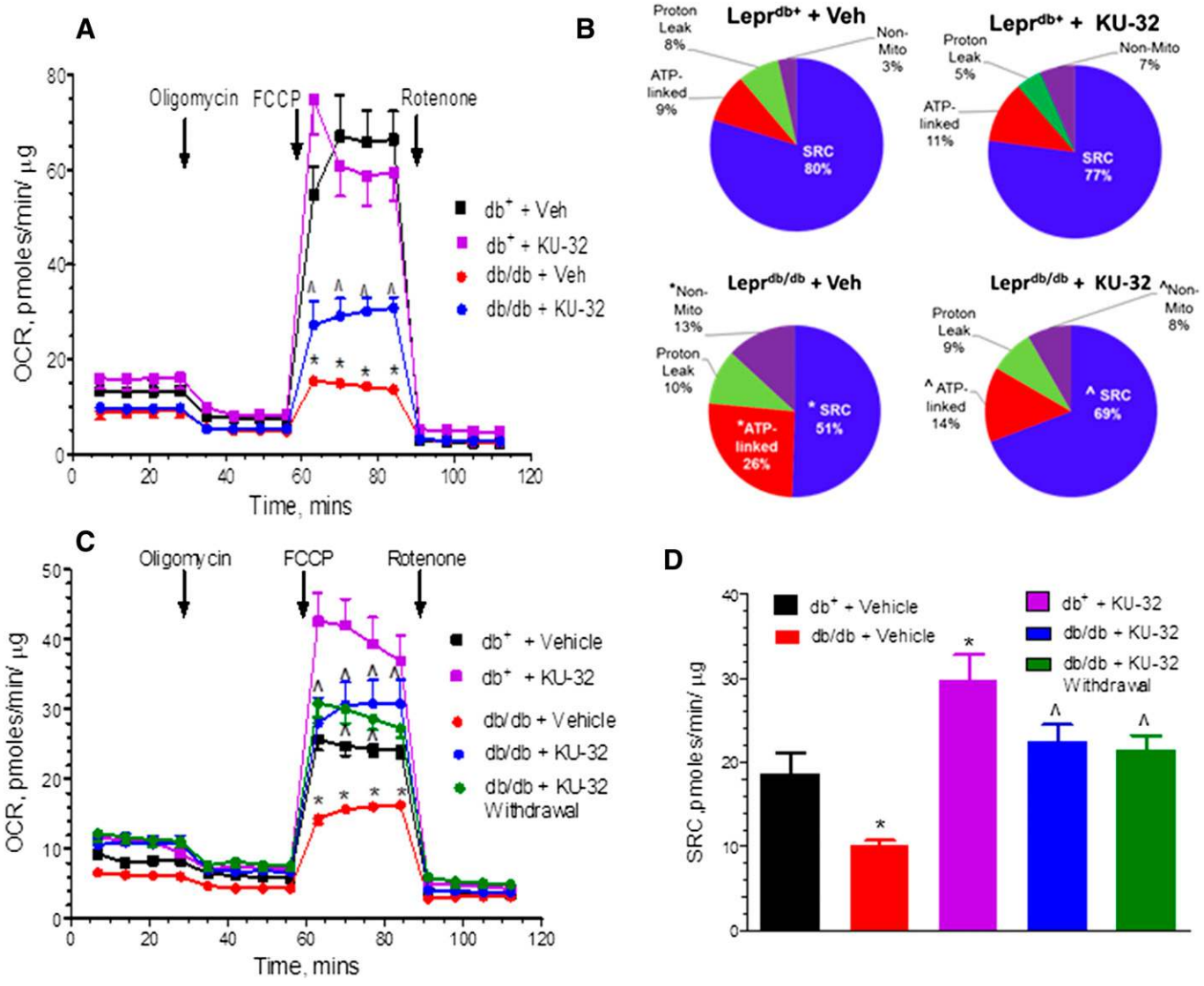

Fig. 4. KU-32 improves mitochondrial bioenergetics in Lepr$^{db/db}$ mice. Sensory neurons were obtained from 14- (A and B) or 18-week- (C and D) old Lepr$^{db/db}$ and Lepr$^{db/+}$ mice treated with KU-32 or Captisol and prepared for bioenergetic analysis. (A) MRC was significantly impaired in untreated Lepr$^{db/db}$ compared with age-matched Lepr$^{db/+}$ mice, and this deficit was significantly improved by KU-32 treatment. (B) Fourteen-week-old Lepr$^{db/db}$ mice have a significant decrease in SRC and an increase in ATP-linked and nonmitochondrial respiration compared with age-matched Lepr$^{db/+}$ mice, and these parameters were significantly improved by KU-32 therapy. (C) At 18 weeks of age MRC remained significantly impaired in the Lepr$^{db/db}$ compared with age-matched Lepr$^{db/+}$ mice. However, MRC was essentially unchanged from 14-week-old untreated Lepr$^{db/db}$. (D) MRC and SRC remained significantly improved in KU-32 treated Lepr$^{db/db}$ mice regardless of whether the drug was give continuously or withdrawn for the final 4 weeks of the study. In (A–D), *$P < 0.05$ versus Lepr$^{db/+}$ + vehicle (Veh); ^$P < 0.05$ versus Lepr$^{db/db}$ + Veh.

and 4B). The respiratory control ratio (RCR) is an indication that the mitochondria have a high capacity for substrate oxidation and ATP synthesis and a low proton leak (Brand and Nicholls, 2011). At 14 weeks of age, diabetes decreased the RCR from 14.8 ± 1.6 in the $Lepr^{db/+}$ mice to 6.8 ± 0.03 in the untreated $Lepr^{db/db}$ animals. $Lepr^{db/db}$ animals treated for 4 weeks with KU-32 showed a significant improvement in MRC and SRC, and the RCR increased to 12.5 ± 0.5 versus untreated $Lepr^{db/db}$ animals, suggesting that modulating molecular chaperones increased the capacity for mitochondrial substrate oxidation.

Not surprisingly, MRC and SRC remained significantly impaired in the 18-week-old $Lepr^{db/db}$ animals compared with the $Lepr^{db/+}$ mice, and continued therapy with KU-32 improved MRC and SRC, but not really beyond levels observed after 4 weeks of drug administration (Fig. 4, C and D). However, KU-32 therapy exerted a prolonged effect on neuronal mitochondrial function because the improvement in SRC promoted by 4 weeks of KU-32 therapy (Fig. 4B) was maintained 4 weeks after drug administration was terminated (Fig. 4D). This result was similar to the continued increase in nerve electrophysiology that was observed 4 weeks after drug withdrawal.

Lastly, to determine whether the improved bioenergetics might be due to an increase in mitochondrial biogenesis, the levels of cytochrome *b* and cytochrome *c* oxidase subunit II (mitochondrial genes) in the DRG from the 18-week-old mice were assessed by quantitative PCR and normalized to the nuclear gene, β-actin (Santos et al., 2011). The expression of both genes was expressed as the fold of the level present in vehicle-treated $Lepr^{db/+}$ mice. However, no differences were observed in the untreated (1.01 ± 0.08, $n = 3$) or KU-32 treated (0.98 ± 0.06, $n = 4$) $Lepr^{db/db}$ mice.

Diabetes-Induced Hypoalgesia Precedes Decreased Mitochondrial Function in a Model of Type 1 Diabetes

Because it is unclear whether changes in mtBE and sensory function follow similar patterns in type 1 and type 2 diabetes, this was examined using Swiss Webster mice rendered diabetic with STZ (Table 2). By 12 weeks of diabetes, the mice developed a significant mechanical (Fig. 5A) and thermal (Supplemental Fig. 1A) hypoalgesia. However, these early sensory deficits were not associated with a significant impairment in mitochondrial respiration since SRC was significantly impaired only after 16 weeks of diabetes (Fig. 5B).

To determine whether improved sensory function following treatment with KU-32 was linked to an improvement in mtBE, drug therapy was initiated at week 17, and sensory neurons were harvested 1, 3, and 5 weeks after drug administration. Prior to drug treatment, the mice showed significant decreases in nerve conduction velocities (Supplemental Fig. 1B) along with the thermal and mechanical hypoalgesia. Although 1 week of KU-32 administration did not increase the diabetes-induced decline in mitochondrial respiration, continued treatment revealed a tight temporal correlation between an improved SRC (Fig. 5B) and recovery from the mechanical hypoalgesia (Fig. 5C), MNCV (Fig. 5D), and SNCV deficits (Supplemental Fig. 1C).

Hsp70 Is Necessary to Improve Mitochondrial Bioenergetics following KU-32 Therapy

We have shown previously that Hsp70 was necessary for the beneficial effect of KU-32 on improving insensate DPN (Urban et al., 2010). To examine whether the improvement in mtBE also required Hsp70, we compared the effect of KU-32 therapy on WT and Hsp70 KO mice rendered diabetic with STZ (Table 3). Diabetic WT and Hsp70 KO mice developed a mechanical hypoalgesia (Fig. 6, A and B) and MNCV deficits (Fig. 6, C and D). Thermal sensitivity and SNCV responded similarly (Supplemental Fig. 2, A–D). After 12 weeks of diabetes, the sensory deficits were well established, and although initiating weekly KU-32 therapy improved all the sensory endpoints in the WT mice, this response was totally absent in the drug-treated, diabetic, Hsp70 KO mice.

After 15 or 18 weeks of diabetes, MRC (Fig. 7, A and B) and SRC (Fig. 7, C and D) showed a similar decline in WT and Hsp70 KO mice. Thus, Hsp70 does not contribute to the

TABLE 2
Weight, FBG, and HbA_{1c} of Swiss Webster mice

Week	Treatment	Weight	FBG	HbA_{1c}	*n*
		g	*mg/dl*	*% (mol/mol)*[a]	
10	Veh + Veh	34.1 ± 2.5	127 ± 12	—	4
	STZ + Veh	27.3 ± 1.1	540 ± 96*	—	4
12	Veh + Veh	34.0 ± 1.7	122 ± 10	5.0 ± 0.4 (31 ± 4.4)	6
	STZ+ Veh	30.3 ± 3.9	600*	12.9 ± 0.2* (117 ± 2.2)	7
16	Veh + Veh	43.0 ± 3.1	117 ± 6	5.4 ± 0.7 (36 ± 7.7)	4
	STZ + Veh	28.6 ± 4.1	573 ± 54*	11.7 ± 0.9* (104 ± 9.8)	4
18	Veh + Veh	43.8 ± 3.1	114 ± 15	4.7 ± 0.2 (28 ± 2.2)	4
	STZ + Veh	29.3 ± 4.2	564 ± 35*	9.9 ± 1.8* (85 ± 19.7)	4
	Veh + KU-32	39.2 ± 2.2	138 ± 18	4.6 ± 0.3 (27 ± 3.3)	4
	STZ + KU-32	30.8 ± 1.7	589 ± 21*	10.7 ± 0.8 * (93 ± 8.7)	4
20	Veh + Veh	40.2 ± 3.9	125 ± 9	4.9 ± 0.2 (30 ± 2.2)	4
	STZ + Veh	32.7 ± 2.8	600*	12.1 ± 0.6* (109 ± 6.6)	4
	Veh + KU-32	41.4 ± 2.6	120 ± 1	5.2 ± 0.6 (33 ± 6.6)	4
	STZ + KU-32	33.0 ± 6.0	600*	12.1 ± 0.9* (109 ± 9.8)	3
22	Veh + Veh	44.0 ± 0.6	123 ± 10	5.1 ± 0.1 (32 ± 1.1)	4
	STZ + Veh	30.3 ± 2.6	600*	10.2 ± 1.7 * (88 ± 18.6)	3
	Veh + KU-32	43.0 ± 2.6	120 ± 1	4.8 ± 0.3 (29 ± 3.3)	4
	STZ + KU-32	35.9 ± 0.9	600*	10.7 ± 1.6 * (93 ± 17.5)	3

Veh, vehicle.
[a]mmol of HbA_{1c}/mol of hemoglobin.
*$P < 0.05$ versus Veh + Veh.

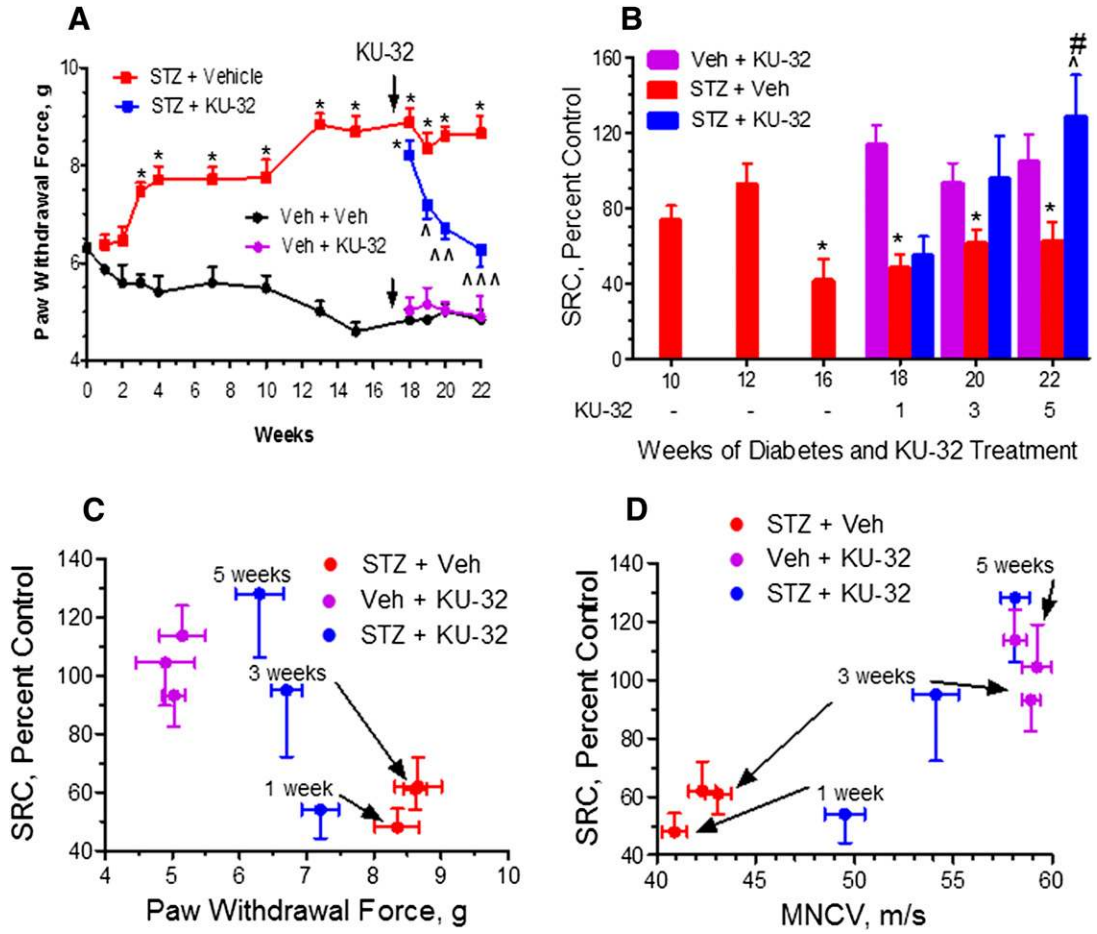

Fig. 5. Sensory hypoalgesia precedes the onset of mitochondrial bioenergetic deficits in a type 1 model of diabetes. Swiss Webster mice were rendered diabetic with STZ, mechanical sensitivity measured at the indicated weeks, and sensory neurons isolated after 10, 12, and 16 weeks of diabetes to assess mitochondrial function. After 17 weeks of diabetes, KU-32 was given weekly and sensory neurons isolated 1, 3, and 5 weeks after drug administration to assess mitochondrial function. (A) Diabetes induced a mechanical hypoalgesia that was maximal after 13 weeks and was reversed by KU-32 treatment. *$P < 0.05$ versus time-matched vehicle (Veh) + Veh; ^$P < 0.05$; ^^$P < 0.01$; ^^^$P < 0.001$, versus time-matched STZ + Veh for all P values. (B) SRC was significantly decreased after 16 weeks of diabetes, and initiation of KU-32 therapy led to a time-dependent recovery of SRC that correlated with improvements in mechanical hypoalgesia (C) and MNCV (D). *$P < 0.05$ versus Veh + Veh; ^$P < 0.05$ versus STZ + Veh; #$P < 0.05$ versus STZ + 1 week KU-32.

diabetes-induced decline in mtBE. On the other hand, 3–6 weeks of KU-32 therapy improved MRC and SRC in diabetic WT mice but neither respiratory parameter was altered by the drug in diabetic Hsp70 KO mice. Importantly, the lack of efficacy of KU-32 in the Hsp70 KO mice is unlikely to result from differences in drug uptake or metabolism, since similar levels of KU-32 were present in DRG, sciatic nerve, and foot pads of WT and Hsp70 KO mice (data not shown). These data

TABLE 3
Weight, FBG, and HbA_{1c} of C57Bl/6 and Hsp70 KO mice

Weeks	Treatment	C57Bl/6				Hsp70 KO			
		Weight	FBG	HbA_{1c}	n	Weight	FBG	HbA_{1c}	n
		g	*mg/dl*	*% (mmol/mol)*[a]		*g*	*mg/dl*	*% (mmol/mol)*[a]	
15	Veh + Veh	28.6 ± 3.4	149 ± 38	4.7 ± 0.2 (28 ± 2.2)	12	25.9 ± 3.1	137 ± 38	4.6 ± 0.2 (27 ± 2.2)	7
	STZ + Veh	20.7 ± 3.8	546 ± 75*	9.9 ± 1.58 (85 ± 17)	9	22.9 ± 3.4	431 ± 114*	8.7 ± 1.8* (72 ± 19.7)	6
	Veh + KU-32	24.4 ± 2.8	163 ± 47	4.5 ± 0.2 (26 ± 2.2)	12	24.2 ± 2.9	133 ± 18	4.6 ± 0.3 (27 ± 3.3)	8
	STZ + KU-32	21.6 ± 2.9	506 ± 98*	8.0 ± 1.5* (64 ± 17)	8	23.6 ± 3.9	478 ± 68*	8.4 ± 1.2* (68 ± 13.1)	5
18	Veh + Veh	25.5 ± 1.5	163 ± 45	4.7 ± 0.1 (28 ± 1.1)	4	23.7 ± 3.1	127 ± 15	5.0 ± 0.1 (31 ± 1.1)	8
	STZ + Veh	25.0 ± 2.7	419 ± 104*	8.2 ± 0.7* (66 ± 7.7)	3	25.4 ± 2.7	457 ± 66*	9.9 ± 0.9* (85 ± 9.8)	5
	Veh + KU-32	27.0 ± 0.6	151 ± 18	4.8 ± 0.2 (29 ± 2.2)	4	25.3 ± 2.3	141 ± 20	4.8 ± 0.3 (29 ± 3.3)	7
	STZ + KU-32	24.0 ± 2.2	415 ± 161*	8.5 ± 1.9* (69 ± 21)	3	22.9 ± 2.9	413 ± 57*	9.9 ± 1.8* (85 ± 19.7)	6

Veh, vehicle.
[a]mmol of HbA_{1c}/mol of hemoglobin.
*$P < 0.05$ versus Veh + Veh.

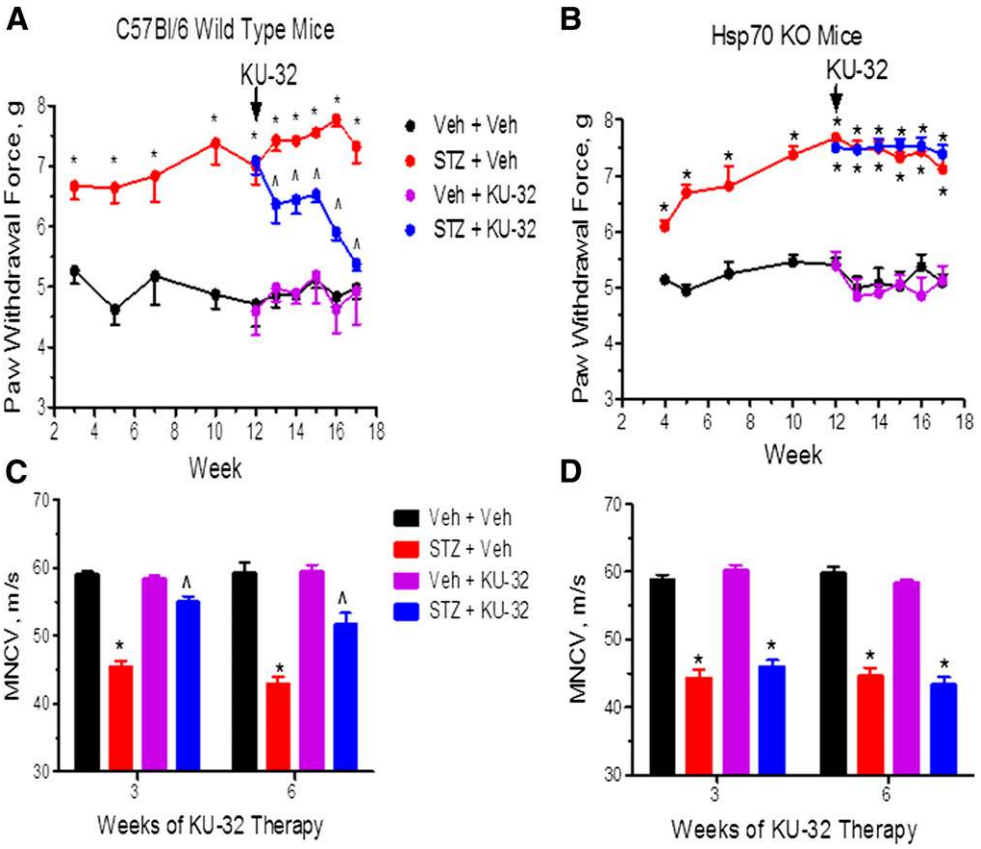

Fig. 6. Hsp70 is necessary for KU-32 to reverse DPN. C57Bl/6 wild type (A and C) and Hsp70 KO (B and D) mice were rendered diabetic with STZ and after 12 weeks of diabetes, KU-32 was given weekly for 6 weeks. Mechanical sensitivity (A and B) was assessed at the indicated weeks and MNCV (C and D) was assessed after 18 weeks of diabetes. In all panels, $*P < 0.05$ versus time-matched vehicle (Veh) + Veh; $\wedge P < 0.05$ versus time-matched STZ + Veh.

support the conclusion that Hsp70 is required to improve mtBE and sensory function following KU-32 therapy.

Discussion

Mitochondrial Dysfunction and the Onset of DPN in Type 2 Diabetes. Similar to previous results in models of type 1 diabetes (Chowdhury et al., 2012; Urban et al., 2012), we observed deficits in multiple bioenergetic parameters in sensory neurons obtained from Lepr$^{db/db}$ animals, a genetic model of type 2 diabetes. Although prior results have clearly implicated mitochondrial dysfunction in the development of insensate DPN in type 1 diabetes (Fernyhough et al., 2010; Chowdhury et al., 2013), our results are the first to temporally link the kinetics of onset of the bioenergetic deficits with the developing hypoalgesia in a model of type 2 diabetes.

The Lepr$^{db/db}$ mice showed significant deficits in MRC and SRC 4–6 weeks after the onset of hyperglycemia, which correlated with the rapidly developing sensory hypoalgesia. MRC measures the rate of maximal electron transport activity and substrate oxidation that the sensory neurons can achieve in the absence of limitations imposed by the proton gradient across the inner mitochondrial membrane. The decrease in MRC suggests that electron transport in the diabetic mitochondria was impaired or that availability of substrates such as glucose and pyruvate was limiting. Although substrate availability might be affected by decreased activity of glycolysis and the tricarboxylic acid cycle as observed in 24-week-old Lepr$^{db/db}$ mice (Hinder et al., 2013b), the rate of extracellular acidification, a measure of glycolytic activity, was relatively similar between the Lepr$^{db/db}$ and Lepr$^{db/+}$ mice (data not shown). The similar levels of extracellular acidification suggest that the deficit in ATP production is either not sufficient to stimulate glycolysis or the diabetic neurons do not effectively revert to glycolysis to help produce ATP. Indeed, as observed by others (Chowdhury et al., 2012), the percent of the basal OCR that was attributable to ATP-linked respiration increased in the 10–18-week-old Lepr$^{db/db}$ compared with the Lepr$^{db/+}$ mice. Presumably, since the maximal rate of electron transport and substrate oxidation is compromised in the diabetic neurons, a greater portion of total respiration is commitment toward ATP-production to meet cellular demands.

SRC provides an indication of how close a cell is functioning to its bioenergetic limit (Sansbury et al., 2011). The progressive decline in SRC suggests that the diabetic neurons have a diminished energetic reserve to respond to the continued metabolic challenges associated with the chronic hyperglycemia and dyslipidemia in the Lepr$^{db/db}$ mice. Because KU-32 significantly improved SRC and NCV even after 4 weeks of drug withdrawal, moderate improvements in respiratory function via modulating chaperones may have long-term benefits for nerve electrophysiology. For example, decreased Na^+/K^+ ATPase activity is associated with slowing of MNCV in DPN (Coppey et al., 2001), and improved mitochondrial function may contribute to ameliorating this deficit.

Lastly, an unexpected outcome of our study was the significant improvement in SRC in the nondiabetic Lepr$^{db/+}$ mice treated with KU-32 for 8 weeks. The underlying reason for this improvement is unclear but may be related to the decreased mitochondrial respiratory capacity that was observed in the vehicle-treated 18-week-old Lepr$^{db/+}$ mice

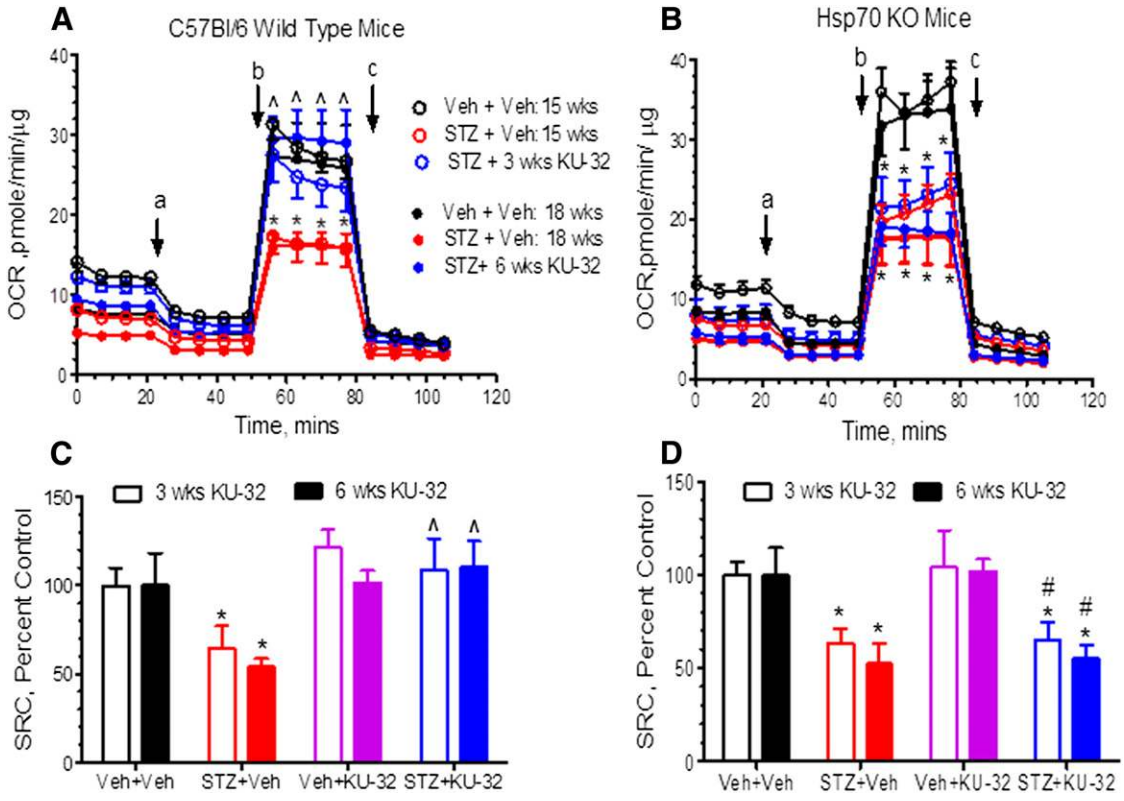

Fig. 7. Hsp70 is necessary for KU-32 to improve mitochondrial bioenergetics. C57Bl/6 wild-type (A and C) and Hsp70 KO (B and D) mice were rendered diabetic with STZ and after 12 weeks of diabetes, KU-32 was given weekly for 6 weeks. Sensory neurons were isolated 3 and 6 weeks after drug administration to assess mtBE. Diabetes decreased MRC (A and B) and SRC (C and D) in both C57Bl/6 and Hsp70 KO, but KU-32 therapy only improved these deficits in the diabetic C57Bl/6 mice. Oligomycin, FCCP, and rotenone/antimycin were injected at the times indicated by a, b, and c, respectively. *$P < 0.05$ versus vehicle (Veh) + Veh; ^$P < 0.05$ versus STZ + Veh; #$P < 0.05$ versus C57Bl/6 STZ + KU-32.

(compare black squares in Fig. 4, A and C). The decreased respiratory capacity between untreated 14- and 18-week-old $Lepr^{db/+}$ mice was observed in the testing of two separate groups of animals from different litters and suggests that the *Lepr* mutation may have an age-related effect on mitochondrial function.

Mitochondrial Dysfunction and the Onset of DPN in Type 1 Diabetes. In the type 1 model, diabetic mice developed a mechanical and thermal hypoalgesia between 6–12 weeks in the absence of significant decreases in SRC. However, mitochondrial respiration was significantly reduced after 16 weeks of diabetes. These data suggest that a fundamental difference may exist in the temporal role of altered mtBE in contributing to the early onset of hypoalgesia in type 1 versus type 2 diabetes. Because both models showed relatively similar levels of hyperglycemia, differences in the kinetics of onset of the bioenergetic decline may be influenced by insulin resistance, which is coincident with mitochondrial dysfunction in tissues such as oxidative skeletal muscle and liver of the $Lepr^{db/db}$ mice (Holmstrom et al., 2012). Alternatively, dyslipidemia is often associated with type 2 diabetes and has been suggested to contribute to DPN (Vincent et al., 2009). However, genetic deletion of apolipoprotein E to increase dyslipidemia in $Lepr^{db/db}$ mice did not exacerbate DPN assessed at 6 months of age (Hinder et al., 2013a), suggesting that dyslipidemia may not significantly worsen sensory neuron mitochondrial dysfunction in type 2 diabetes.

Modulating Hsp70 Improves mtBE and DPN. Although the onset of a thermal and mechanical hypoalgesia does not require a significant change in mtBE in the type 1 model, the improvement in the psychosensory and electrophysiologic measures of nerve function in both diabetic animal models tightly correlated with an increase in mtBE following KU-32 therapy. The absence of this correlation in the diabetic Hsp70 KO mice provides the first evidence that modulating Hsp70 is a necessary effector for KU-32 to improve the bioenergetic profile of the sensory neurons and nerve function. This benefit was unrelated to any effect of KU-32 or Hsp70 on improving glucose disposal or any of the metabolic parameters in either model. However, a clear limitation of this work is that although a tight, Hsp70-dependent correlation exists between improved mtBE and the various measures of nerve function, a causal relationship between them is not established. Thus, we cannot rule out that Hsp70 may have independent and parallel effects on mtBE and other targets that contribute to improving psychosensory and electrophysiologic function following KU-32 therapy.

Although the etiology of DPN is not attributed to the accumulation of a specific misfolded or aggregated protein, the efficacy of Hsp70 in improving mtBE suggests that diabetic mitochondria are undergoing some level of proteotoxic stress. Because KU-32 can decrease oxidative stress and increase mitochondrial and cytosolic chaperones in

hyperglycemically stressed primary sensory neurons, these factors may directly contribute to improving mtBE and SRC in diabetic mice (Zhang et al., 2012). In this regard, hyperglycemia can increase oxidative stress and the oxidative modification of amino acids (Akude et al., 2010) that may impair protein folding within mitochondria (Muchowski and Wacker, 2005), decrease mitochondrial protein import (Baseler et al., 2011), and promote mitochondrial dysfunction (Tomlinson and Gardiner, 2008). In the mitochondrial proteome, ~99% of the proteins are imported into the organelle and Hsp70 serves as a chaperone for hydrophobic precursors of inner mitochondrial membrane proteins (Schmidt et al., 2010). Because Hsp70 is not a resident mitochondrial chaperone, determining whether it might mitigate diabetes-induced dysfunction in mtBE by facilitating the import, removal, and/or replacement of damaged mitochondrial proteins is an important biologic question with clear therapeutic relevance to treating DPN.

The reliance on Hsp70 for the tight correlation between improved mtBE and the physiologic measures of DPN adds to the evidence that modulating molecular chaperones may benefit various neurodegenerative diseases where mitochondrial respiratory function is compromised (Ouyang et al., 2006; Xu et al., 2010). However, it may be critical to limit the extent of Hsp70 induction since overexpression of Hsp70 in HeLa cells inhibited oxidative phosphorylation and augmented anaerobic glycolysis (Wang et al., 2012). As certain malignant phenotypes are characterized by Hsp70 overexpression and increased glycolytic rates, the efficacy of modulating Hsp70 to enhance neuronal mtBE might rely on pharmacologic agents that are weak or cell-selective inducers of Hsp70. Although glycolytic activity decreases in diabetic nerve (Hinder et al., 2013b), additional work will be needed to determine if long-term modulation of Hsp70 might negatively affect neuronal oxidative phosphorylation and be a liability in treating DPN.

In summary, numerous approaches toward treating insensate DPN have centered on inhibiting specific pathogenic pathways linked to glucotoxicity, with limited translational success (Calcutt et al., 2009). The pharmacologic management of insensate DPN is difficult since no single etiologic event has been unequivocally identified to contribute to disease development in a temporally and/or biochemically uniform fashion over the long natural history of the disease. Since pharmacologic modulation of endogenous neuroprotective chaperones does not rely on targeting a specific pathogenic enzyme (i.e., aldose reductase) or pathway (i.e., oxidative stress) that contributes to DPN, it provides a venue to complement etiocentric therapies. Coupled with close attention toward obtaining glycemic goals, modulating molecular chaperones may aid the medical management of DPN in patients with type 1 and type 2 diabetes.

Acknowledgments

The authors thank Jillisa Molanari and Joanna Krise for technical support in performing the qPCR and the LC MS/MS analyses, respectively.

Authorship Contributions

Participated in research design: Dobrowsky, Ma, Farmer.
Conducted experiments: Ma, Farmer, Pan, Urban.
Contributed new reagents or analytic tools: Zhao, Blagg.
Performed data analysis: Ma, Farmer, Pan, Urban, Dobrowsky.
Wrote or contributed to the writing of the manuscript: Dobrowsky, Ma, Farmer.

References

Akude E, Zherebitskaya E, Chowdhury SKR, Smith DR, Dobrowsky RT, and Fernyhough P (2011) Diminished superoxide generation is associated with respiratory chain dysfunction and changes in the mitochondrial proteome of sensory neurons from diabetic rats. *Diabetes* **60**:288–297.
Akude E, Zherebitskaya E, Roy Chowdhury SK, Girling K, and Fernyhough P (2010) 4-Hydroxy-2-nonenal induces mitochondrial dysfunction and aberrant axonal outgrowth in adult sensory neurons that mimics features of diabetic neuropathy. *Neurotox Res* **17**:28–38.
Baseler WA, Dabkowski ER, Williamson CL, Croston TL, Thapa D, Powell MJ, Razunguzwa TT, and Hollander JM (2011) Proteomic alterations of distinct mitochondrial subpopulations in the type 1 diabetic heart: contribution of protein import dysfunction. *Am J Physiol Regul Integr Comp Physiol* **300**:R186–R200.
Brand MD and Nicholls DG (2011) Assessing mitochondrial dysfunction in cells. *Biochem J* **435**:297–312.
Calcutt NA, Cooper ME, Kern TS, and Schmidt AM (2009) Therapies for hyperglycaemia-induced diabetic complications: from animal models to clinical trials. *Nat Rev Drug Discov* **8**:417–429.
Callaghan BC, Cheng HT, Stables CL, Smith AL, and Feldman EL (2012) Diabetic neuropathy: clinical manifestations and current treatments. *Lancet Neurol* **11**: 521–534.
Chowdhury SK, Zherebitskaya E, Smith DR, Akude E, Chattopadhyay S, Jolivalt CG, Calcutt NA, and Fernyhough P (2010) Mitochondrial respiratory chain dysfunction in dorsal root ganglia of streptozotocin-induced diabetic rats and its correction by insulin treatment. *Diabetes* **59**:1082–1091.
Chowdhury SKR, Smith DR, and Fernyhough P (2013) The role of aberrant mitochondrial bioenergetics in diabetic neuropathy. *Neurobiol Dis* **51**:56–65.
Chowdhury SKR, Smith DR, Saleh A, Schapansky J, Marquez A, Gomes S, Akude E, Morrow D, Calcutt NA, and Fernyhough P (2012) Impaired AMP-activated protein kinase signaling in dorsal root ganglia neurons is linked to mitochondrial dysfunction and peripheral neuropathy in diabetes. *Brain* **135**:1751–1766.
Coppey LJ, Davidson EP, Rinehart TW, Gellett JS, Oltman CL, Lund DD, and Yorek MA (2006) ACE inhibitor or angiotensin II receptor antagonist attenuates diabetic neuropathy in streptozotocin-induced diabetic rats. *Diabetes* **55**:341–348.
Coppey LJ, Gellett JS, Davidson EP, Dunlap JA, Lund DD, and Yorek MA (2001) Effect of antioxidant treatment of streptozotocin-induced diabetic rats on endoneurial blood flow, motor nerve conduction velocity, and vascular reactivity of epineurial arterioles of the sciatic nerve. *Diabetes* **50**:1927–1937.
Delree P, Leprince P, Schoenen J, and Moonen G (1989) Purification and culture of adult rat dorsal root ganglia neurons. *J Neurosci Res* **23**:198–206.
Evans CG, Chang L, and Gestwicki JE (2010) Heat shock protein 70 (Hsp70) as an emerging drug target. *J Med Chem* **53**:4585–4602.
Farmer KL, Li C, and Dobrowsky RT (2012) Diabetic peripheral neuropathy: should a chaperone accompany our therapeutic approach? *Pharmacol Rev* **64**:880–900.
Fernyhough P, Roy Chowdhury SK, and Schmidt RE (2010) Mitochondrial stress and the pathogenesis of diabetic neuropathy. *Expert Rev Endocrinol Metab* **5**:39–49.
Hinder LM, Vincent AM, Hayes JM, McLean LL, and Feldman EL (2013a) Apolipoprotein E knockout as the basis for mouse models of dyslipidemia-induced neuropathy. *Exp Neurol* **239**:102–110.
Hinder LM, Vivekanandan-Giri A, McLean LL, Pennathur S, and Feldman EL (2013b) Decreased glycolytic and tricarboxylic acid cycle intermediates coincide with peripheral nervous system oxidative stress in a murine model of type 2 diabetes. *J Endocrinol* **216**:1–11.
Holmström MH, Iglesias-Gutierrez E, Zierath JR, and Garcia-Roves PM (2012) Tissue-specific control of mitochondrial respiration in obesity-related insulin resistance and diabetes. *Am J Physiol Endocrinol Metab* **302**:E731–E739.
Huang TJ, Price SA, Chilton L, Calcutt NA, Tomlinson DR, Verkhratsky A, and Fernyhough P (2003) Insulin prevents depolarization of the mitochondrial inner membrane in sensory neurons of type 1 diabetic rats in the presence of sustained hyperglycemia. *Diabetes* **52**:2129–2136.
Huang TJ, Verkhratsky A, and Fernyhough P (2005) Insulin enhances mitochondrial inner membrane potential and increases ATP levels through phosphoinositide 3-kinase in adult sensory neurons. *Mol Cell Neurosci* **28**:42–54.
Huang Y-T and Blagg BSJ (2007) A library of noviosylated coumarin analogues. *J Org Chem* **72**:3609–3613.
Jack MM, Ryals JM, and Wright DE (2011) Characterisation of glyoxalase I in a streptozocin-induced mouse model of diabetes with painful and insensate neuropathy. *Diabetologia* **54**:2174–2182.
Li C, Ma J, Zhao H, Blagg BSJ, and Dobrowsky RT (2012) Induction of heat shock protein 70 (Hsp70) prevents neuregulin-induced demyelination by enhancing the proteasomal clearance of c-jun. *ASN Neuro* **4**:e00102.
Matts RL, Brandt GE, Lu Y, Dixit A, Mollapour M, Wang S, Donnelly AC, Neckers L, Verkhivker G, and Blagg BS (2011) A systematic protocol for the characterization of Hsp90 modulators. *Bioorg Med Chem* **19**:684–692.
McGuire JF, Rouen S, Siegfreid E, Wright DE, and Dobrowsky RT (2009) Caveolin-1 and altered neuregulin signaling contribute to the pathophysiological progression of diabetic peripheral neuropathy. *Diabetes* **58**:2677–2686.
Morimoto RI (2011) The heat shock response: systems biology of proteotoxic stress in aging and disease. *Cold Spring Harb Symp Quant Biol* **76**:91–99.
Muchowski PJ and Wacker JL (2005) Modulation of neurodegeneration by molecular chaperones. *Nat Rev Neurosci* **6**:11–22.
Oltman CL, Davidson EP, Coppey LJ, Kleinschmidt TL, Lund DD, Adebara ET, and Yorek MA (2008) Vascular and neural dysfunction in Zucker diabetic fatty rats: a difficult condition to reverse. *Diabetes Obes Metab* **10**:64–74.
Ouyang YB, Xu LJ, Sun YJ, and Giffard RG (2006) Overexpression of inducible heat shock protein 70 and its mutants in astrocytes is associated with maintenance of

mitochondrial physiology during glucose deprivation stress. *Cell Stress Chaperones* **11**:180–186.
Peterson LB and Blagg BS (2009) To fold or not to fold: modulation and consequences of Hsp90 inhibition. *Future Med Chem* **1**:267–283.
Sansbury BE, Jones SP, Riggs DW, Darley-Usmar VM, and Hill BG (2011) Bioenergetic function in cardiovascular cells: the importance of the reserve capacity and its biological regulation. *Chem Biol Interact* **191**:288–295.
Santos JM, Tewari S, Goldberg AFX, and Kowluru RA (2011) Mitochondrial biogenesis and the development of diabetic retinopathy. *Free Radic Biol Med* **51**:1849–1860.
Schmidt O, Pfanner N, and Meisinger C (2010) Mitochondrial protein import: from proteomics to functional mechanisms. *Nat Rev Mol Cell Biol* **11**:655–667.
Tomlinson DR and Gardiner NJ (2008) Glucose neurotoxicity. *Nat Rev Neurosci* **9**:36–45.
Urban MJ, Li C, Yu C, Lu Y, Krise JM, McIntosh MP, Rajewski RA, Blagg BSJ, and Dobrowsky RT (2010) Inhibiting heat-shock protein 90 reverses sensory hypoalgesia in diabetic mice. *ASN Neuro* **2**:e00040.
Urban MJ, Pan P, Farmer KL, Zhao H, Blagg BS, and Dobrowsky RT (2012) Modulating molecular chaperones improves sensory fiber recovery and mitochondrial function in diabetic peripheral neuropathy. *Exp Neurol* **235**:388–396.
Vincent AM, Hayes JM, McLean LL, Vivekanandan-Giri A, Pennathur S, and Feldman EL (2009) Dyslipidemia-induced neuropathy in mice: the role of oxLDL/LOX-1. *Diabetes* **58**:2376–2385.
Wang L, Schumann U, Liu Y, Prokopchuk O, and Steinacker JM (2012) Heat shock protein 70 (Hsp70) inhibits oxidative phosphorylation and compensates ATP balance through enhanced glycolytic activity. *J Appl Physiol* **113**:1669–1676.
Wright DE, Johnson MS, Arnett MG, Smittkamp SE, and Ryals JM (2007) Selective changes in nocifensive behavior despite normal cutaneous axon innervation in leptin receptor-null mutant (db/db) mice. *J Peripher Nerv Syst* **12**:250–261.
Xu L, Emery JF, Ouyang Y-B, Voloboueva LA, and Giffard RG (2010) Astrocyte targeted overexpression of Hsp72 or SOD2 reduces neuronal vulnerability to forebrain ischemia. *Glia* **58**:1042–1049.
Zhang L, Zhao H, Blagg BS, and Dobrowsky RT (2012) C-terminal heat shock protein 90 inhibitor decreases hyperglycemia-induced oxidative stress and improves mitochondrial bioenergetics in sensory neurons. *J Proteome Res* **11**:2581–2593.
Zhao H, Michaelis ML, and Blagg BS (2012) Hsp90 modulation for the treatment of Alzheimer's disease. *Adv Pharmacol* **64**:1–25.

Address correspondence to: Rick T. Dobrowsky, Department of Pharmacology and Toxicology, University of Kansas, 5064 Malott Hall, 1251 Wescoe Hall Dr., Lawrence, KS 66045. E-mail: dobrowsky@ku.edu